EFFECT OF GRINDING PARAMETERS ON SURFACE ROUGHNESS AND CUTTING FORCE WHEN SURFACE GRINDING 90CrSi STEEL BY HAI DUONG GRINDING WHEEL

Luu Anh Tung[1*], Nguyen Ngoc Thieu[1], Ha Toan Thang[2]
[1]TNU - University of Technology, [2]Vietnam-Korea College of Technology in Bac Giang

ARTICLE INFO

Received: 15/01/2024
Revised: 14/5/2024
Published: 14/5/2024

KEYWORDS

Surface grinding
90CrSi steel
Full factorial design
Hai Duong grinding wheel
Annova

ABSTRACT

The parameters of the cutting mode and the cooling lubrication regime play an important role in determining the efficiency and quality of the surface grinding process. In this study, the full factorial design (2^k) was used to investigate the effect of grinding parameters of the cutting mode and the cooling lubrication regime on the surface roughness and the normal force when surface grinding 90CrSi steel by Hai Duong grinding wheel. Minitab 19 software is used to design the L32 experiment with 5 input parameters: cooling flow (LL), coolant concentration (ND), feed rate (S_d), table speed (V_B) and grinding depth (t). The analysis results show that the interaction between ND, S_d and V_B has the greatest influence on the surface roughness (Ra) after grinding, while the depth of cut has the greatest influence on the normal force (Fy). In addition, a regression model determining surface roughness and normal force has been proposed. These results can be applied directly in production, helping to select products, improve product quality and reduce related costs.

ẢNH HƯỞNG CỦA MỘT SỐ THÔNG SỐ QUÁ TRÌNH ĐẾN NHÁM BỀ MẶT VÀ LỰC CẮT KHI MÀI PHẲNG THÉP 90CrSi QUA TÔI BẰNG ĐÁ MÀI HẢI DƯƠNG

Lưu Anh Tùng[1*], Nguyễn Ngọc Thiệu[1], Hà Toàn Thắng[2]
[1]Trường Đại học Kỹ thuật Công nghiệp - ĐH Thái Nguyên, [2]Trường Cao đẳng Công nghệ Việt – Hàn Bắc Giang

THÔNG TIN BÀI BÁO

Ngày nhận bài: 15/01/2024
Ngày hoàn thiện: 14/5/2024
Ngày đăng: 14/5/2024

TỪ KHÓA

Mài phẳng
Thép 90CrSi
Thiết kế thí nghiệm đầy đủ
Đá mài Hải Dương
Phân tích phương sai

TÓM TẮT

Các thông số của chế độ cắt và chế độ trơn nguội đóng vai trò quan trọng trong việc xác định hiệu quả và chất lượng của quá trình mài phẳng. Trong nghiên cứu này, thí nghiệm đầy đủ (2^k) được sử dụng để khảo sát ảnh hưởng của một số thông số công nghệ của chế độ cắt và chế độ bôi trơn làm mát đến nhám bề mặt và lực cắt pháp tuyến khi mài phẳng thép 90CrSi qua tôi bằng đá mài Hải Dương. Phần mềm Minitab 19 được sử dụng để thiết kế thí nghiệm L32 với 5 thông số đầu vào là lưu lượng làm mát (LL), nồng độ dung dịch làm mát (ND), lượng chạy dao dọc (S_d), vận tốc bàn máy (V_B) và chiều sâu mài (t). Kết quả phân tích cho thấy tương tác giữa ND, S_d và V_B có ảnh hưởng lớn nhất đến nhám bề (Ra) mặt sau khi mài, trong khi chiều sâu cắt ảnh hưởng lớn nhất đến lực cắt pháp tuyến (Fy). Ngoài ra, mô hình hồi quy xác định nhám bề mặt và lực cắt pháp tuyến đã được đề xuất. Những kết quả này có thể áp dụng trực tiếp trong sản xuất, giúp lựa chọn, cải thiện chất lượng sản phẩm và giảm chi phí liên quan.

DOI: https://doi.org/10.34238/tnu-jst.9598

* Corresponding author. *Email: luuanhtung@tnut.edu.vn*

1. Introduction

Grinding is a process that is primarily influenced by heat [1]. The temperature in the cutting zone during grinding can reach a range of 1000°C to 1500°C [2]. At this temperature, a range of surface imperfections may arise in the machined parts following grinding. These include microcracks caused by tensile residual stress, material softening due to carbon release, and surface layer burning, among others. Hence, the thermal energy that enters the workpiece needs to be swiftly dissipated using a suitable coolant lubrication system. In addition, the choice of a suitable cutting regimen also has a vital impact. In addition to cooling the workpiece, the cooling of the grinding wheel (particularly crucial for diamond or resin-bonded grinding wheels) diminishes friction, removes debris from the machining area, and cleans the grinding wheel, thereby improving the surface quality of the machined components [1]. Multiple coolant types and cutting strategies have been examined using various techniques to introduce coolants into the grinding area.

In their study, E.J. da Silva and colleagues [3] performed high-speed grinding experiments on 52100 bearing steel using CBN grinding wheels. They used four different types of coolants: 20% synthetic vegetable oil, water, 3% synthetic vegetable oil, and neat oil. The purpose of the study was to assess the wear of the grinding wheel and the surface roughness after machining, with a material removal rate of 6764 mm^3/mm. In their study, S. Shaji and V. Radhakrishnan [4] investigated the grinding process of carbon steel and bearing steel. They examined three different coolant environments: dry, flood with 5% oil-based coolant, and CaF2-oil-based grinding aid. An investigation was conducted to examine the impact of these coolant environments on cutting forces, the ratio of Fz to Fy, surface roughness, and cutting heat. There has been a significant research focus on the introduction of coolant into the cutting zone and the various types of coolants used in flat grinding, driven by the growing trend of environmental protection. Some of the coolants that have garnered considerable research interest include Minimum Quantity Lubrication (MQL) [1], [5] – [11], water [4], dry [4], [8], [12], vegetable-based emulsion [13], and environmentally friendly coolant [14]. Nevertheless, flood cooling remains extensively employed because of its straightforward implementation, offering superior efficiency while satisfying technical specifications.

Moreover, the cutting process employed during grinding has also garnered significant attention from numerous researchers. Mustafa Kemal Külekci [15] employed the Taguchi method to minimize surface roughness while grinding flat AISI 1040 steel with EKR46K grinding wheels. This was achieved by optimizing cutting speed, table speed, and depth of cut. Binu Thomas and colleagues [16] conducted an optimization study on the cutting parameters for grinding SiC ceramic material with a grit size of 320. They used diamond grinding wheels and employed model analysis and experimentation to ensure the desired surface roughness. Therefore, the speed of the grinding wheel, the depth of cut, and the speed of the table have a significant impact on the surface roughness after grinding and show similar patterns [17]. Subrata Talapatra and Ishat Islam [18] utilized the Taguchi method to optimize the material hardness, table speed, and depth of cut in the grinding process of 52100 bearing steel with WA36G5VBE aluminum oxide grinding wheels. Their objective was to minimize surface roughness. Periyasamy et al. [19] employed Response Surface Methodology (RSM) to optimize the feed rate, depth of cut, and dressing depth for grinding AISI 1080 steel with A60V5V grinding wheels. Furthermore, several inquiries have concentrated on identifying the most suitable parameters for the grinding process, including the determination of grinding wheel speed, table speed, dressing depth, and so on, for flat grinding [20] – [23], cylindrical grinding [24] – [26], and external cylindrical grinding [27], [28]. In addition, researchers have also investigated multi-objective optimization for the flat grinding process [29] – [31].

The above analysis shows that the cutting mode and the cooling lubrication regime have received a lot of attention from researchers. However, studies almost exclusively focus on the

cutting mode or the cooling lubrication regime. Research on the simultaneous impact of both the cutting mode and the cooling lubrication regime on surface roughness and normal shear force during grinding has not received enough attention. This paper presents the results of 32 experiments (L32) that aimed to examine the impact of grinding parameters on surface roughness and cutting force during the surface grinding of 90CrSi steel using the Hai Duong grinding wheel.

2. Experiments setup

In order to assess the impact of various technological factors on the surface roughness and tangential cutting force during the grinding of flat 90CrSi steel using Hai Duong grinding stones, a full 2^k experiment was designed using Minitab 19 software. The specific experimental conditions are outlined in Table 1. The coolant concentration has a range of values as recommended by the manufacturer and other parameters have a range of values currently in use at the Precision Mechanical Engineering Enterprise, Thai Ha company. The experiment utilizes a 90CrSi alloy steel tooling material that has undergone heat treatment to achieve a hardness level of 55-58 HRC. The chemical composition of the material is provided in Table 2. The specimen measures 100 millimeters in length, 60 millimeters in width, and 25 millimeters in height. Furthermore, the experimental arrangement is illustrated in Figure 1.

The study selected five input parameters: coolant concentration ND (%), coolant flow rate LL (liters/minute), longitudinal tool feed S_d (mm/single pass), table speed V_B (m/minute), and grinding depth t (mm). The levels and respective values of these parameters are displayed in Table 3. The experimental matrix L32 (25) is depicted in Table 4.

Table 1. *The experimental conditions for surface grinding 90CrSi steel*

Grinding machine	Moto-Yokohama – Japan
Grinding wheel	Cn46TB2GV1.300.32.127.30 m/s – Hai Duong, Vietnam (Figure 2)
Rotation speed of grinding wheel	1800 rev/min
Metalworking lubricants	Caltex Aquatex 3180
Lubricant method	Flood
Dresser	Multi diamond dresser, 3908-0088C, type 2 - Russia
Dressing modes	3 times with a depth of 0.02 mm, 1 time with a depth of 0.01 mm with the same feed rate of 1.6 m/min
Flow measurement instrument	Z-5615 Panel Flowmeter – Thailand
Surface roughness measuring device	SJ201 – Mitutoyo – Japan
Three Component Dynamometer	Kistler 9257BA – Switzerland

Table 2. *Chemical composition of elements of 90CrSi tool alloy steel*

Chemical composition (%)										
C	Si	Mn	P≤	S≤	Cr≤	Mo≤	Ni≤	V≤	W≤	Others
0.85-0.95	1.2 -1.6	0.3 -0.6	0.03	0.03	0.95 - 1.25	0.2	0.35	0.15	0.2	Cu ≤ 0.3; Ti ≤ 0.03

Table 3. *Levels and corresponding values of experimental input parameters*

Level / Variable	Lowest		Highest	
	Real	**Encode**	**Real**	**Encode**
Coolant flow LL (lit/min)	10	-1	20	+1
Coolant concentration ND [%]	3	-1	5	+1
Cross feed S_d [mm/strock]	8	-1	12	+1
Table speed V_B [m/min]	8	-1	12	+1
Depth of cut t [mm]	0.01	-1	0.02	+1

Following the establishment of the system, experiments were systematically conducted in a predetermined sequence within the same machine run at the Precision Mechanical Engineering Enterprise, Thai Ha company. The Kistler 9257BA was used to measure the normal cutting force

Fy during the 3rd grinding cycle (Figure 3). The surface roughness was measured using the SJ201 roughness measuring device after the third grinding cycle (Figure 4). The experiment was conducted three times. The surface roughness value and cutting force are calculated as the mean of three experimental runs, as illustrated in Table 5.

Table 4. *Arrange experimental matrix L32 (2^5)*

StdOrder	RunOrder	CenterPt	Blocks	LL [lit/min]	ND [%]	S_d [mm/strock]	V_B [m/min]	t [mm]
28	1	1	1	20	5	8	12	0.02
3	2	1	1	10	5	8	8	0.01
5	3	1	1	10	3	12	8	0.01
27	4	1	1	10	5	8	12	0.02
…								
6	31	1	1	20	3	12	8	0.01
17	32	1	1	10	3	8	8	0.02

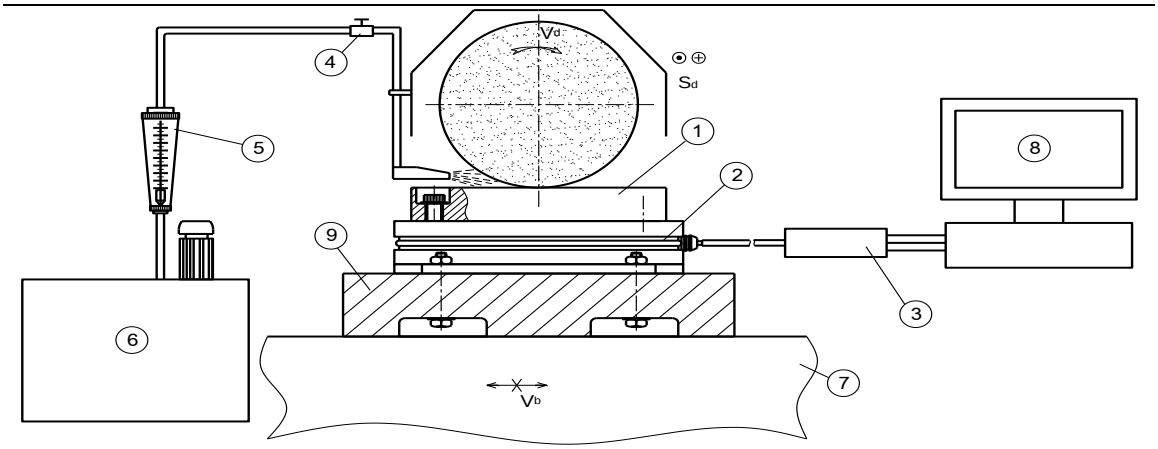

Figure 1. *Experimental setup*

1 – Workpiece
2 – Kistler 9257BA
3 – Adapter
4 – Flow control valve
5 – Flow measurement instrument
6 – Coolant container
7 – Magnetic table
8 – Computer

3. Results and discussion

3.1. Identify the main influencing factors

The qualitative determination of the experimental parameters that primarily influence the surface roughness Ra and the normal cutting force Fy is achieved through the utilization of the main effects graph (Figure 5).

In Figure 5a, five graphs illustrating the impact of 5 input parameters are displayed in five distinct boxes, specifically regarding the surface roughness Ra. The upper-left quadrant of the graph illustrates the impact of the LL parameter. Upon examining the graph, it can be observed that as the value of LL changes from 10 lit/min to 20 lit/min, the objective function Ra undergoes a variation from 0.617 μm to 0.586 μm. The gradient of this graph is calculated by subtracting the y-coordinates (0.617 - 0.586) and dividing the result by the difference in x-coordinates, which is 2. Therefore, the slope of the graph is 0.0155. The slopes of Ra with respect to changes in ND, S_d, V_B, and t are as follows: 0.041, 0.007, 0.014, and 0.012, respectively. The qualitative comparison reveals that the ND graph has the highest slope, followed by LL, V_B, t, and finally S_d. Hence, it is clear that ND exerts the most significant impact, whereas S_d has the least significant impact on the objective function of surface roughness, Ra.

Table 5. *Results of measuring surface roughness and normal cutting force of experimental L32*

StdOrder	RunOrder	CenterPt	Blocks	LL	ND	S_d	V_B	t	Ra [μm]	Fy [N]
28	1	1	1	20	5	8	12	0.02	0.496	141.7
3	2	1	1	10	5	8	8	0.01	0.893	65
5	3	1	1	10	3	12	8	0.01	0.616	93.3
27	4	1	1	10	5	8	12	0.02	0.606	166.7
32	5	1	1	20	5	12	12	0.02	0.752	183.3
25	6	1	1	10	3	8	12	0.02	0.546	146.7
15	7	1	1	10	5	12	12	0.01	0.687	99.7
16	8	1	1	20	5	12	12	0.01	0.663	110.7
22	9	1	1	20	3	12	8	0.02	0.67	151
4	10	1	1	20	5	8	8	0.01	0.609	76.7
20	11	1	1	20	5	8	8	0.02	0.774	121.7
18	12	1	1	20	3	8	8	0.02	0.416	105
24	13	1	1	20	5	12	8	0.02	0.63	154.3
13	14	1	1	10	3	12	12	0.01	0.546	97.7
8	15	1	1	20	5	12	8	0.01	0.449	86
9	16	1	1	10	3	8	12	0.01	0.549	102.7
26	17	1	1	20	3	8	12	0.02	0.638	142.3
2	18	1	1	20	3	8	8	0.01	0.444	67.3
1	19	1	1	10	3	8	8	0.01	0.44	51.3
21	20	1	1	10	3	12	8	0.02	0.583	145
12	21	1	1	20	5	8	12	0.01	0.428	89.7
11	22	1	1	10	5	8	12	0.01	0.796	119
7	23	1	1	10	5	12	8	0.01	0.51	88.3
19	24	1	1	10	5	8	8	0.02	0.815	105
30	25	1	1	20	3	12	12	0.02	0.605	159.3
14	26	1	1	20	3	12	12	0.01	0.611	100.7
29	27	1	1	10	3	12	12	0.02	0.665	148.3
31	28	1	1	10	5	12	12	0.02	0.649	131.7
23	29	1	1	10	5	12	8	0.02	0.514	152
10	30	1	1	20	3	8	12	0.01	0.604	81.7
6	31	1	1	20	3	12	8	0.01	0.583	85.7
17	32	1	1	10	3	8	8	0.02	0.452	91.7

In Figure 5b, the slopes of the objective function Fy with respect to changes in LL, ND, S_d, V_B, and t are 1.652, 3.806, 9.775, 11.957, and 25.944, respectively. Upon qualitative comparison, it is evident that the graph's slope with respect to the parameter t is the highest, followed by V_B, S_d, ND, and finally LL. Therefore, the variable t has the most significant impact, while LL has the least significant impact on the Fy objective function.

The data presented in Figures 5a and 5b clearly show that there is a direct relationship between the flow rate and surface roughness, where an increase in flow rate leads to an increase in surface roughness. Additionally, there is an inverse relationship between the flow rate and cutting force, where an increase in flow rate results in a decrease in cutting force. An augmentation in the coolant concentration, feed rate, table speed, and depth of cut all results in an escalation of both surface roughness and cutting force. To clarify, the following explanation can be provided: An augmentation in the rate of fluid movement diminishes the effectiveness of the cooling lubricant, resulting in an escalation of the force exerted during cutting and a reduction in the smoothness of the surface. An increased coolant concentration leads to a thickening of the coolant, which in turn reduces its ability to escape. This results in an elevation of both cutting force and surface roughness. Augmenting the feed rate leads to an expansion of the cutting area, which refers to the contact between the cutting tool and the workpiece surface. This expansion

causes the cutting layer to widen, resulting in an escalation of cutting force and surface roughness. Increasing the table speed decreases the duration of contact between the grinding wheel and the workpiece, resulting in higher cutting force and surface roughness. Augmenting the magnitude of the cut enhances the thickness of the layer being cut, resulting in an escalation of both the force exerted during cutting and the unevenness of the surface.

Figure 2. *The geometry of the grinding wheel used in the experiment*

Figure 4. *Image of surface roughness measurement results*

Figure 3. *The actual connection measures the cutting force*

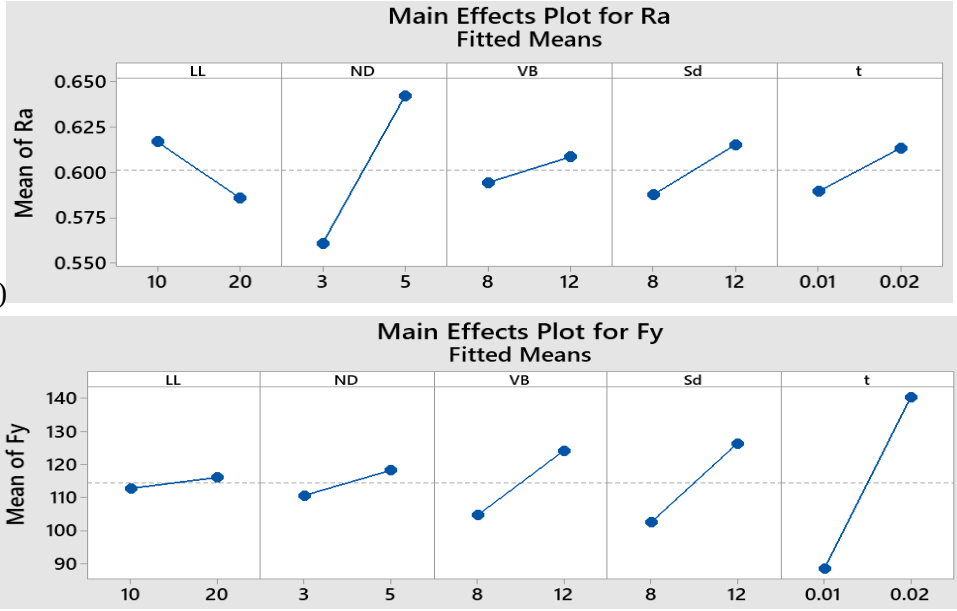

a)

b)

Figure 5. *Graph of main effects of factors LL, ND, S_d, V_B, t to: a) Surface roughness Ra; b) Normal shear force Fy*

Figure 6 exhibits the standardized influence diagrams for the surface roughness Ra (Figure 6a) and the tangential cutting force Fy (Figure 6b) with a significance level of α = 0.05. Red square points represent parameters that have a significant influence. In Figure 3a, the parameters that have a significant impact on Ra are: B (parameter ND), interaction AB (interaction between LL*ND), AC (interaction between LL*S_d), AE (interaction between LL*t), BC (interaction between ND*S_d), BD (interaction between ND*V_B), CD (interaction between S_d*V_B), ABC (interaction between LL*ND*S_d), ABE (interaction between LL*ND*t), BCD (interaction between ND*S_d*V_B). Figure 3b illustrates the parameters that have a significant impact on Fy, specifically: B (parameter ND), C (parameter S_d), D (parameter V_B), E (parameter t), interaction CD (interaction between S_d*V_B), ACD (interaction between LL*S_d*V_B).

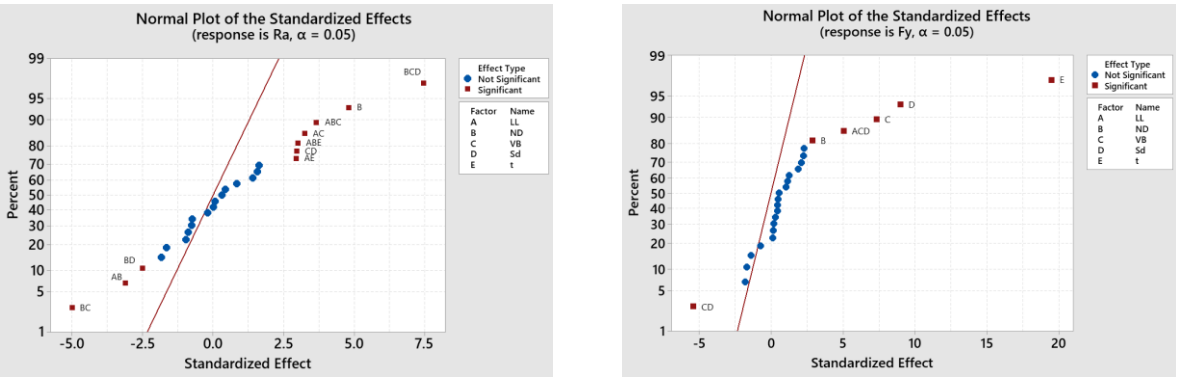

a) *b)*

Figure 6. *Normalized influence graph of factors LL, ND, S_d, V_B, t to a) Surface roughness Ra; b) Normal shear force Fy*

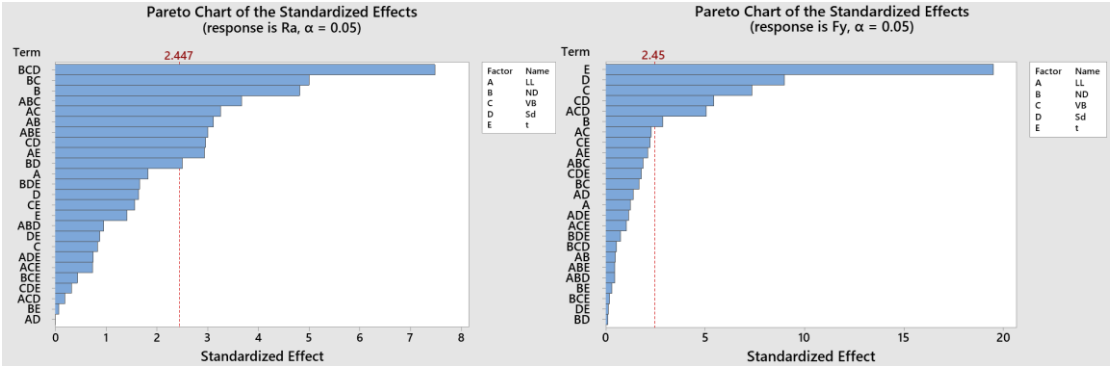

a) *b)*

Figure 7. *Pareto graph of influencing factors LL, ND, S_d, V_B, t to: a) Surface roughness Ra; b) Normal shear force F_y*

The Pareto chart of influencing factors is employed to ascertain the hierarchy of parameters and their interactions on the surface roughness Ra and the tangential cutting force Fy (Figure 7). The standardized influence values are depicted as horizontal bars. Parameters that correspond to bars that extend beyond the right limit line are deemed to have a significant influence. Individuals situated to the left of the limit line are regarded as having lower levels of influence. In Figure 7a, the interaction BCD (ND*S_d*V_B) has the most significant influence on surface roughness Ra, followed by BC (interaction ND*S_d), B (ND), ABC (interaction LL*ND*S_d), AC (interaction LL*S_d), AB (interaction LL*ND), ABE (interaction LL*ND*t), CD (interaction S_d*V_B), AE (interaction LL*t), and finally BD (interaction ND*t). Figure 7b depicts: The depth of cut parameter E has the most significant influence on the tangential cutting force Fy, followed by the table speed parameter D, the feed rate parameter C, the interaction parameter ACD (LL*V_B*S_d), and finally the coolant concentration parameter B.

3.2. Variance regression analysis

The results of variance analysis for parameters affecting surface roughness Ra and tangential cutting force Fy are shown in Tables 6 and 7, after removing insignificant influential factors and interactions.

Table 6. *Analyze the variance of the regression model after removing factors that have a weak influence on surface roughness Ra*

Source	DF	Seq SS	Adj MS	F-Value	P-Value	C (%)
Linear	5	0.073041	0.01461	6.38	0.022	16.48
LL	1	0.007657	0.00766	3.34	0.117	1.73
ND	1	0.053057	0.05306	23.18	0.003	11.97
S_d	1	0.00161	0.00161	0.7	0.434	0.36
V_B	1	0.006133	0.00613	2.68	0.153	1.38
t	1	0.004584	0.00458	2	0.207	1.03
2-Way Interactions	7	0.158004	0.02257	7.22	0.012	35.65
LL*ND	1	0.022208	0.02221	9.7	0.021	5.01
LL*S_d	1	0.024255	0.02426	10.6	0.017	5.47
LL*t	1	0.01985	0.01985	8.67	0.026	4.48
ND*S_d	1	0.057207	0.05721	24.99	0.002	12.91
ND*V_B	1	0.014323	0.01432	6.26	0.046	3.23
ND*t	1	0.000011	1.1E-05	0	0.946	0.00
S_d*V_B	1	0.02015	0.02015	8.8	0.025	4.55
3-Way Interactions	3	0.179361	0.05979	8.35	0.009	40.47
LL*ND*S_d	1	0.030814	0.03081	13.46	0.01	6.95
LL*ND*t	1	0.020655	0.02066	9.02	0.024	4.66
ND*S_d*V_B	1	0.127892	0.12789	55.87	0	28.86
Error	16	0.032764	0.00205			7.39
Total	31	0.443169				100.00

Model Summary

S	R-sq	R-sq(adj)	R-sq(pred)
0.0452521	92.61%	85.68%	70.43%

Table 7. *Analysis of variance of the regression model after removing factors that weakly affect the normal shear force Fy*

Source	DF	Seq SS	Adj MS	F-Value	P-Value	C (%)
Linear	5	29722	5944.4	104.89	0	85.18
LL	1	87.8	87.8	1.55	0.26	0.25
ND	1	463.6	463.6	8.18	0.029	1.33
S_d	1	3057.6	3057.6	53.95	0	8.76
V_B	1	4574.5	4574.5	80.72	0	13.11
t	1	21538.5	21538.5	380.04	0	61.73
2-Way Interactions	3	2071.1	690.367	4.92	0.032	5.94
LL*S_d	1	294	294	5.19	0.063	0.84
LL*V_B	1	109.5	109.5	1.93	0.214	0.31
S_d*V_B	1	1667.5	1667.5	29.42	0.002	4.78
3-Way Interactions	1	1452.6	1452.6	3.6	0.065	4.16
LL*S_d*V_B	1	1452.6	1452.6	25.63	0.002	4.16
Error	22	1647.5	74.8864			4.72
Total	31	34893.1				100.00

Model Summary

S	R-sq	R-sq(adj)	R-sq(pred)
8.65359	95.28%	93.35%	90.01%

Table 6 shows that among the main factors, only the coolant concentration parameter ND has a significant effect on the surface roughness Ra, with a p-value of 0.003. Although other parameters do not have a direct impact on the Ra objective, they do have a significant influence on the interactions between two parameters and the interactions between three parameters. The factors being examined demonstrate significant two-way interaction effects, with p-values less than 0.046, except for the ND*t interaction which has a p-value of 0.942. However, this interaction is still included to assess the three-way interaction. All of the introduced three-way interactions exhibit p-values that are very small (less than 0.024), indicating statistical significance in the influence of these interactions. Put simply, both the main influences and the interaction effects that were studied are statistically significant.

Table 7 shows that the main effects have p-values that are very small (less than 0.029), indicating that they have a statistically significant influence. Although the remaining parameters do not have a direct and significant impact on the Fy objective, they do exhibit a strong influence in the context of three-dimensional interactions. The interaction effects between the factors have extremely small p-values (less than 0.000), except for the LL*S_d interaction (p = 0.063) and S_d*V_B (p = 0.214), which are included in the analysis to determine the three-way interaction. All of the introduced three-way interactions have p-values less than 0.002, indicating their statistically significant interaction effects. This suggests that both the primary effects and the interaction effects being examined are highly significant.

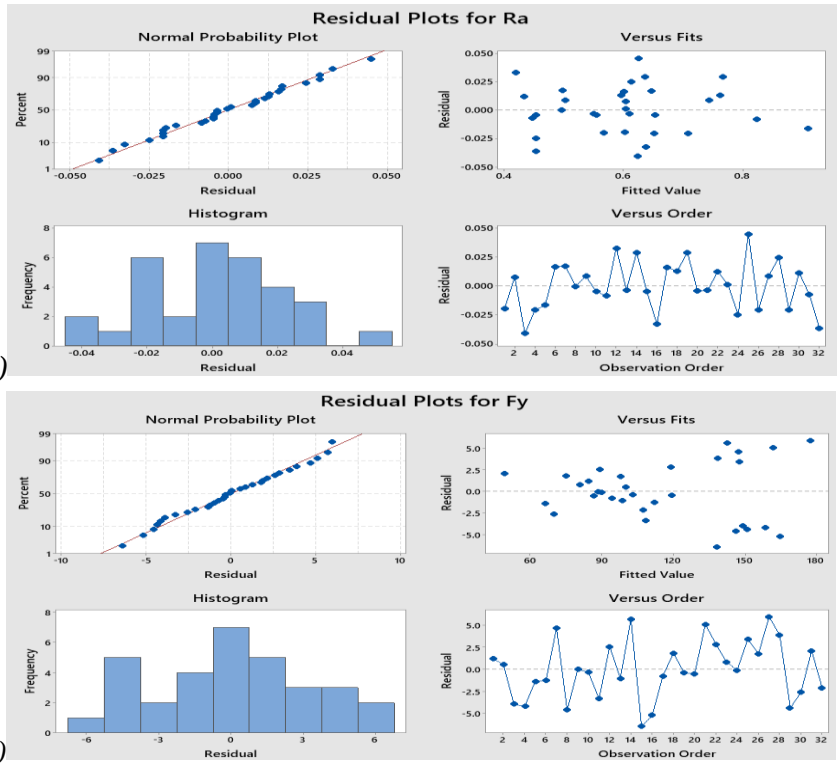

a)

b)

Figure 8. *Graphs evaluate the surplus for: a) Surface roughness Ra; b) Normal shear force F_y*

3.3. Regression model

Minitab 19 software is utilised to propose regression equations for the determination of Ra and Fy. Tables 6 and 7 demonstrate that the R-squared and adjusted R-squared values of the regression models are exceptionally high (92.61% and 95.25% respectively), indicating a strong alignment between the equations and the data. The proposed models for calculating Ra and Fy are as follows (1) and (2).

3.4. Evaluate the residuals of the regression model

Figure 8 displays the residual assessment plots for Ra and Fy. The Normal Probability Plot juxtaposes the probability distribution of residuals (represented by dots) with the normal distribution (represented by a continuous straight line). The plot demonstrates that residuals exhibit a high degree of proximity to the normal distribution. The Histogram plot displays the frequency at which residuals occur. The Versus Fit plot depicts the association between residuals and the corresponding values of the regression model. The presence of randomly distributed points, without any discernible pattern, suggests that the Ra and Fy data inputs are independent of any controlled factors, except for the chosen parameters. The Versus Order plot illustrates the correlation between residuals and the sequential arrangement of data points. The presence of randomly scattered points, devoid of any identifiable pattern, indicates that the Ra and Fy data inputs are unaffected by temporal influences.

$$\begin{aligned} Ra = {} & -7.39 + 0.0825\,LL + 2.434\,ND + 0.785\,S_d + 0.477\,V_B - 23.2\,t - 0.0434\,LL*ND \\ & - 0.00700\,LL*S_d + 0.00594\,LL*V_B - 0.56\,LL*t - 0.2313\,ND*S_d - 0.1354\,ND*V_B - \\ & 4.8\,ND*t - 0.0578\,S_d*V_B + 0.34\,S_d*t + 5.42\,V_B*t + 0.003103\,LL*ND*S_d - \\ & 0.000809\,LL*ND*V_B + 1.016\,LL*ND*t - 0.000080\,LL*S_d*V_B - 0.124\,LL*S_d*t - \\ & 0.127\,LL*V_B*t + 0.01580\,ND*S_d*V_B + 0.372\,ND*S_d*t - 1.403\,ND*V_B*t + 0.136\,S_d*V_B*t \end{aligned} \quad (1)$$

$$\begin{aligned} Fy = {} & -905 + 53.1\,LL + 70.4\,ND + 81.0\,S_d + 70.7\,V_B - 4684\,t - 3.32\,LL*ND - 4.474\,LL*S_d - \\ & 4.251\,LL*V_B - 561\,LL*t - 7.08\,ND*S_d - 1.16\,ND*V_B + 440\,ND*t - 5.79\,S_d*V_B \\ & + 978\,S_d*t + 1146\,V_B*t + 0.250\,LL*ND*S_d + 0.059\,LL*ND*V_B + 23.8\,LL*ND*t \\ & + 0.3369\,LL*Sd*V_B + 27.3\,LL*S_d*t + 30.6\,LL*V_B*t + 0.181\,ND*S_d*V_B \\ & + 26\,ND*S_d*t - 98\,ND*V_B*t - 119.4\,S_d*V_B*t \end{aligned} \quad (2)$$

4. Conclusion

This paper reports the results of a study investigating the impact of specific cutting and coolant conditions on the surface roughness and tangential cutting force (Fy) during the grinding process of 90CrSi steel using Hai Duong grinding wheels. A total of 32 experiments (L32) were conducted using an experimental design. The findings demonstrate that the coolant concentration has a substantial impact on both Ra and Fy. However, other parameters individually show varying levels of influence or insignificance on Ra or Fy. Nevertheless, the interactions between these parameters have noteworthy effects on the objectives. Additionally, a regression model has been suggested for the estimation of Ra and Fy. When the R-squared values surpass 92.61%, it can be concluded that the proposed model is appropriate for use.

Acknowledgment

This paper was supported by Thai Nguyen University of Technology, Thai Nguyen University.

REFERENCES

[1] V. P. Astakhov and S. Joksch, *Metalworking fluids (MWFs) for cutting and grinding - Fundamentals and recent advances*, Woodhead Publishing Limited, 2012.

[2] F. Klocke, *Manufacturing processes 2 – Grinding, honing, lapping*, Springer, 2009.

[3] S. M. Alves, E. J da Silva, and J. F. G. de Oliveira, "Analysis of the influence of different cutting fluids in the wear of cbn wheel in high speed grinding," *17th International congress of mechanical engineering*, November, 2003, pp. 10-14.

[4] S. Shaji and V. Radhakrishnan, "A study on calcium fluoride as a solid lubricant in grinding," *International Journal of Environmentally Conscious Design & Manufacturing*, vol. 11, pp. 29-36, 2023.

[5] B. B. Fathallah and N. B. Fredj, "Effects of abrasive type cooling mode and peripheral grinding wheel speed on the AISI D2 steel ground surface integrity," *International Journal of Machine Tools & Manufacture*, vol. 49, pp. 261–272, 2009.

[6] J. A. Sanchez and I. Pombo, "Machining evaluation of a hybrid MQL-CO2 grinding technology," *Journal of Cleaner Production*, vol. 18, pp. 1840-1849, 2010.

[7] L. R. D. Silva and E. C. Bianchi, "Analysis of surface integrity for minimum quantity lubricant-MQL in grinding," *International Journal of Machine Tools & Manufacture*, vol. 47, pp. 412–418, 2007.

[8] N. B. Fredj, H. Sidhom, and C. Braham, "Ground surface improvement of the austenitic stainless steel AISI304 using cryogenic cooling," *Surface & Coatings Technology*, vol. 200, pp. 4846-4860, 2006.
[9] R. Alberdi and J. A. Sanchez, "Strategies for optimal use of fluids in grinding," *International Journal of Machine Tools & Manufacture*, vol. 51, pp. 491–499, 2011.
[10] S. K. Patra and S. Swain, "Effects of minimum quantity lubrication (MQL) in grinding: Principle, applications and recent advancements," *Materials Today: Proceedings*, vol. 69, Part 2, pp. 96-106, 2022.
[11] B. K. Sato, J. C. Lopes, F. S. F. Ribeiro, R. L. Rodriguez, B. B. Domingues, H. A. D. Souza, L. E. D. A. Sanchez, and E. C. Bianchi, "Evaluating the effect of MQL technique in grinding VP50IM steel with green carbide wheel," *The International Journal of Advanced Manufacturing Technology*, vol. 121, pp. 7287–7294, 2022.
[12] B. Mandal, R. Singh, S. Das, and S. Banerjee, "Improving grinding performance by controlling air flow around a grinding wheel," *International Journal of Machine Tools & Manufacture*, vol. 51, pp. 670–676, 2011.
[13] R. Y. Fusse and T. V. Franca, "Analysis of the Cutting Fluid Influence on the Deep Grinding Process with a CBN Grinding Wheel," *Materials Research*, vol. 7, no. 3, pp. 451-457, 2004.
[14] T. Nguyen and L. C. Zhang, "The coolant penetration in grinding with a segmented wheel-Part 2: Quantitative analysis," *International Journal of Machine Tools & Manufacture*, vol. 46, pp. 114–121, 2006.
[15] M. K. Külekci, "Analysis of process parameters for a surface-grinding process based on the Taguchi method," *Materiali in tehnologije/ Materials and technology*, vol.47, pp. 105–109, 2013.
[16] B. Thomas, E. David, and R. Manu, "Modeling and optimization of surface roughness in surface grinding of SiC advanced ceramic material," *5th International & 26th All India Manufacturing Technology, Design and Research Conference (AIMTDR 2014)*, IIT Guwahati, Assam, India, December 12th –14th, 2014, pp. 667-696.
[17] E. I. Suzdaltsev, A. S. Khamitsaev, A. G. Épov, and D. V. Kharitonov, "Regimes of Mechanical Grinding of Pyroceramic Components in the System Machine – Workpiece – Tool – Scheme," *Refractories and Industrial Ceramics*, vol. 45, no. 1, pp.10-15, 2004.
[18] S. Talapatra and I. Islam, "Optimization of grinding parameters for minimum surface roughness using Taguchi method," *International Conference on Mechanical, Industrial and Energy Engineering*, Khulna, Bangladesh, December 25-26, 2014, pp. 1-6.
[19] D. S. Periyasamy, M. Aravind, D. Vivek, and D. K. S. Amirthagadeswaran, "Optimization of surface grinding process parameters for minimum surface roughness in AISI 1080 using Response Surface Methodology," *Advanced Materials Research*, vol. 984-985, pp. 118-123, 2014.
[20] D. Pai, S. Shrikantha, and R. R. D'Souza, "Multi objective optimization of surface grinding process by combination of Response surface methodology and Enhanced non-dominated sorting genetic algorithm," *International Journal of Computer Applications (0975 – 8887)*, vol. 36, no. 3, pp. 19-24, 2011.
[21] G. Warnecke and C. Barth, "Optimization of the Dynamic Behavior of Grinding Wheels for Grinding of Hard and Brittle Materials Using the Finite Element Method," *CIRP Annals - Manufacturing Technology*, vol. 48, no. 1, pp. 261-264, 1999.
[22] J. S. Kwak and M. K. Ha, "Evaluation of Wheel Life by Grinding Ratio and Static Force," *KSME International Journal*, vol. 16, no. 9, pp. 1072-1077, 2002.
[23] H. Yan, F. Deng, Z. Qin, J. Zhu, H. Chang, and H. Niu, "Effects of Grinding Parameters on the Processing Temperature," *Crack Propagation and Residual Stress in Silicon Nitride Ceramics. Micro-machines*, vol. 14, 2023, Art. no. 666, doi: 10.3390/mi14030666.
[24] G. Xiao and S. Malkin, "On-Line Optimization for Internal Plunge Grinding," *CIRP Annals - Manufacturing Technology*, vol. 45, no. 1, pp. 287-292, 1996.
[25] H. K. Tönshoff, M. Zinngrebe, and M. Kemmerling, "Optimization of Internal Grinding by Microcomputer-Based Force Control," *CIRP Annals- Manufacturing Technology*, vol. 35, no. 1, pp. 293-296, 1986.
[26] I. Inasaki, "Monitoring and Optimization of Internal Grinding Process," *CIRP Annals - Manufacturing Technology*, vol. 40, no. 1, pp. 359-362, 1991.
[27] Y. C. Fu, H. J. Xu, and J. H. Xu, "Optimization design of grinding wheel topography for high efficiency grinding," *Journal of Materials Processing Technology*, vol. 129, no. 1-3, pp. 118-122, 2002.
[28] K. R. Jagtap, S. B. Ubale, and D. M. S.Kadam, "Optimization of cylindrical grinding process parameters for AISI 5120 steel using taguchi method," *International Journal of Design and Manufacturing Technology (IJDMT)*, vol. 2, pp. 47-56, 2011.
[29] Asokan, N. Baskar, K. Babu, G. Prabhaharan, and R. Saravanan, "Optimization of surface grinding operations using Particle Swarm Optimization technique," *Journal of Manufacturing Science and Engineering*, vol. 127, pp. 885-892, 2025.
[30] P. J. Pawar, R. V. Rao, and J. P. Davim, "Multiobjective optimization of grinding process parameters using particle swarm optimization algorithm," *Materials and Manufacturing Processes*, vol. 25, pp. 424–431, 2010.
[31] G. Zhang, M. Liu, J. Li, and W. Y. Ming, "Multi-objective optimization for surface grinding process using a hybrid particle swarm optimization algorithm," *Int. J. Adv. Manuf. Technol.*, vol. 71, pp. 1861–1872, 2014.